

Probing the halo structure of the 2^- excited state of ^{10}Be
through a *halo-to-halo* transfer reaction

January 9, 2023

J. Chen¹, P. Capel², A. Obertelli³, V. Durant², Y. Ayyad⁴, F. Browne⁵, R. Gernhaeuser⁶,
C. R. Hoffman¹, T. Kröll³, W. P. Liu⁷, J. L. Lou⁸, D. K. Sharp⁹, K. Wimmer¹⁰,
H. Y. Zhu⁸, B. L. Xia⁸, H. Y. Ge⁸

¹*Physics Division, Argonne National Laboratory, Argonne, IL 60439, USA*

²*Institut für Kernphysik, Johannes Gutenberg-Universität at Mainz, D-55099 Mainz, Germany*

³*Institut für Kernphysik, Technische Universität Darmstadt, 64289 Darmstadt, Germany*

⁴*Instituto de Estructura de la Materia, CSIC, E-28006 Madrid, Spain*

⁵*ISOLDE, CERN, CH-1211 Geneva 23, Switzerland*

⁶*Physics Department, Technical University of Munich, 85748 Garching, Germany*

⁷*College of Science, Southern University of Science and Technology, Shenzhen, China.*

⁸*School of Physics and State Key Laboratory of Nuclear Physics and Technology, Peking University, Beijing 100871, China*

⁹*Department of Physics and Astronomy, University of Manchester, Manchester M13 9PL, UK*

¹⁰*GSI Helmholtzzentrum für Schwerionenforschung GmbH, Planckstr. 1, D-64291 Darmstadt, Germany*

Spokespersons: J. Chen [jiechenphysics@gmail.com], P. Capel, A. Obertelli

Contact person: F. Browne

Abstract: The 2^- state in ^{10}Be has been the subject of numerous experimental and theoretical studies because it is supposed to exhibit a one-neutron halo structure. However, experimental results are not consistent and dependent highly on the reaction models and their input parameters. Furthermore, experimental methods to study halos in excited states are so far very limited because of the very short lifetime of these states. To resolve this situation we propose a new experimental method in which a neutron is transferred at very low beam energy from a halo state to the state of interest. The cross section will be significant only if the final state exhibits a one-neutron halo structure. We plan to measure the transfer reaction $^9\text{Be}(^{11}\text{Be}, ^{10}\text{Be})^{10}\text{Be}^*(2^-)$ at 0.61 and 1.22 MeV/u. At these energies, the cross sections will be largely enhanced if the 2^- state exhibits a halo. To achieve this, we request 18 shifts of beam time with 9 shifts for each beam energy. Outgoing charged particles will be detected by a set of silicon detectors and the γ rays will be detected by MINIBALL.

Requested shifts: [18] shifts, (split into [1] runs over [1] years)



Introduction

In the past decades, a number of neutron-rich nuclei have been found to have extended spatial distributions. This phenomenon is known as the *neutron halo* [1, 2]. There are one-neutron halo nuclei, such as ^{11}Be , ^{15}C , and ^{19}C , as well as two-neutron halo nuclei, such as ^6He and ^{11}Li . The halo phenomenon is essentially a weak-binding effect of the valence one or two neutrons, which decouple from the relatively inert core of the nucleus. The concept of halo, however, is not limited to the sole ground state, but can be generalized to loosely bound excited states displaying a single-particle nature with a radially extended distribution. To date, a number of excited halo state candidates have been suggested to exist, but their study is hindered by their very short lifetimes, so they must be searched for as products of reactions or decays.

One of the most extensively discussed candidates for such excited-state halo is the 2^- state (6.263 MeV) in ^{10}Be , which is just 0.549 MeV below the one-neutron separation threshold, and which may exhibit a dominant configuration with one neutron in the $2s_{1/2}$ orbital bound to the $3/2^-$ ground state of ^9Be . Theoretically, both the microscopic multi-cluster and no-core shell model predict an extended matter distribution for that state, with a root-mean-square (rms) radius, $r^{\text{rms}} \sim 6.09$ fm much larger than the ground state's, which hints for a halo structure [3]. Some experiments probed the s -wave spectroscopic factor of this state using one-neutron transfer or knockout reactions but the existing results are not consistent and have large dependences on the optical-model parameters or normalization of the absolute cross sections [4, 5, 6, 7, 8, 9]. Accordingly, there is still no conclusion about the existence of a halo in the 2^- state of ^{10}Be .

We hereby propose a new method to probe the presence of a one-neutron halo in excited states and, in particular, to confirm the halo structure of the 2^- excited state of ^{10}Be . The basic idea behind the method is to perform a transfer reaction at very low energy, below the Coulomb barrier. In this way the cores of the colliding nuclei never come close to each other, and only the tail of their wave functions contribute to the reaction. If the final state exhibits a halo, the cross section should be significantly larger than if it does not. To ensure that the Q value of the reaction stays positive, the valence neutron in the incoming nucleus should also be loosely bound. In addition, to increase the cross section, the magnitude of the tail of its wave function should be as large as possible. Accordingly the projectile should also exhibit a halo. This *halo-to-halo* transfer seems to be the ideal probe of a halo structure in highly excited states of nuclei.

For this experiment, we propose the $^9\text{Be}(^{11}\text{Be},^{10}\text{Be})^{10}\text{Be}^*(2^-)$ transfer from the one-neutron halo nucleus ^{11}Be to the ^9Be target. Our calculations show that the presence of a halo in the 2^- state of ^{10}Be should enhance the cross section by a factor as large as 4 over a non-halo 2^- state. To control the validity of this approach, comparisons can be made to other close-by states in ^{10}Be , which do not exhibit a halo structure. If successful, this method will open wide opportunities for the future experimental study of the halo structure in excited states of nuclei.

Theoretical calculation of the $^9\text{Be}(^{11}\text{Be},^{10}\text{Be})^{10}\text{Be}^*(2^-)$ transfer reaction

To estimate the cross section for that reaction, we consider the following three-body model. The ^{11}Be projectile is seen as a ^{10}Be core in its 0^+ ground state to which a valence neutron is loosely bound in the $s_{1/2}$ orbital. This projectile impinges on a ^9Be target, of which the internal structure is ignored. During the collision, the halo neutron is transferred to the target to form the 2^- excited state of ^{10}Be , which, if it exhibits a halo structure, can be well described as $^9\text{Be}+n$. To compute this three-body collision, we use the Adiabatic Distorted Wave Approximation (ADWA) [10].

To describe the initial and final halo states, we consider Halo EFT [11], which has been shown to work very well to model reactions with halo nuclei [12, 13]. At Leading Order (LO), the sole central Gaussian term of the potential is fitted to the halo-neutron binding energy. Considering different widths σ of that interaction provides different amplitudes of the known exponential asymptotic behavior of the radial core-neutron wave function, i.e. different asymptotic normalization coefficients (ANCs). At Next-to-Leading Order (NLO), Halo-EFT potentials include two terms, which can be used to fit also the ANC. Varying the ANC of the halo state, while keeping the actual binding energy to get the correct Q value of the reaction, enables us to test the influence of the halo on the cross section. This is illustrated in the left panel of Fig. 1, where different ${}^9\text{Be}$ - n radial wave functions are plotted. To describe ${}^{11}\text{Be}$, we consider the NLO wave functions developed in Ref. [12]. The ${}^{10}\text{Be}$ - ${}^9\text{Be}$ core-target interaction is simulated by an optical potential obtained by the double-folding of chiral-EFT NN interactions at $N^2\text{LO}$ [14, 15].

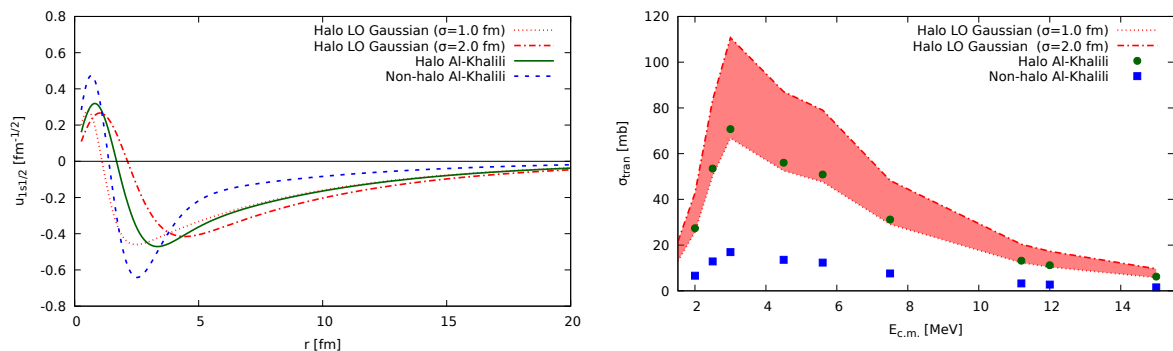


Figure 1: Left: Radial wave functions for the ${}^{10}\text{Be}$ 2^- excited state, obtained with Gaussian ${}^9\text{Be}$ - n binding potentials. The result at LO with $\sigma = 1$ and 2 fm are shown as red dotted and dash-dotted lines, respectively. The ones fitted to the ANC of a halo (ANC = $0.745 \text{ fm}^{-1/2}$) and non-halo (ANC = $0.376 \text{ fm}^{-1/2}$) states of Ref. [3] are shown as the solid green and dashed blue lines, respectively. Right: Integrated transfer cross sections as a function of $E_{c.m.}$. The red band shows the sensitivity to the LO potentials with $\sigma = 1$ (lower line) and 2 fm (upper line). The symbols correspond to results obtained for a 2^- excited state with (green points) and without (blue squares) a one-neutron halo structure.

The right panel of Fig. 1 shows the integrated one-neutron transfer cross sections at different c.m. energies (from 2 to 15 MeV). The red band illustrates the sensitivity of the results to the 2^- state in ${}^{10}\text{Be}$. It has been obtained by changing the width of the Gaussian potential at LO between $\sigma = 1$ and 2 fm (lower and upper lines, respectively). Because the cross section scales nearly perfectly with the ANC of the final state, we can conclude, that the reaction is purely peripheral in the ${}^9\text{Be}$ - n coordinate, in the sense that it depends only on the asymptotics of that wave function. A similar analysis shows that the reaction is also fully peripheral in the ${}^{10}\text{Be}$ - n coordinate of the projectile, confirming what was expected from the semi-classical argument developed in the Introduction. Accordingly, the measurement of that reaction would enable us to determine whether the 2^- excited state in ${}^{10}\text{Be}$ exhibits a halo.

To get a reliable estimate for the cross section, we repeat the calculation with an NLO ${}^9\text{Be}$ - n interaction fitted to reproduce the ANC of $0.745 \text{ fm}^{-1/2}$ inferred from the structure calculation of Al-Khalili and Arai [3] (green solid line in the left panel of Fig. 1). The corresponding cross section, which lies at the bottom of the LO band, is shown by the green dots in the right panel

of the same figure. New *ab initio* calculations within the No Core Shell Model with Continuum model (NCSMC) give an ANC of $0.756 \text{ fm}^{-1/2}$ [16], which is comparable to the value of Ref. [3]. Therefore, the actual value of the transfer cross section should not be far from this estimate.

To test the effect of an absence of halo in that state, we repeat the reaction calculations using a ${}^9\text{Be}-n$ wave function with a reduced ANC of $0.376 \text{ fm}^{-1/2}$ deduced from the calculation of ${}^{10}\text{Be}$ non-halo states [3]. That wave function is shown by the blue dashed line in the left panel of Fig. 1, and the corresponding cross section by the blue squares the right panel. These values are a factor of 4 lower than the green points indicating that, with enough statistics, the presence of a halo in that state can be clearly identified.

Fig. 2 shows the angular distribution of the outgoing nuclei after the neutron transfer at $E_{c.m.} = 3$ and 6 MeV. We choose the former energy because the integrated cross section peaks at about 3 MeV (see Fig. 1). Another measurement at 6 MeV is used to confirm the energy dependence of the reaction. For both energies, the green solid lines correspond to the ${}^{10}\text{Be}^*(2^-)$ halo state, while the dashed blue lines correspond to the non-halo one. For these differential cross sections we see that, at large angles, the cross sections scale as the ANC squared, a clear sign of the peripherality of the reaction. Accordingly, the region of large angles in the c.m. frame would be the region of interest for the measurement.

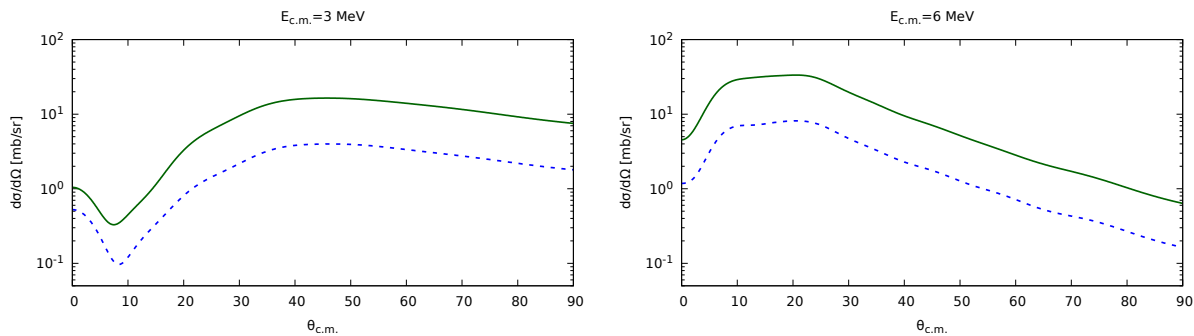


Figure 2: Transfer cross sections as a function of the center-of-mass angle for $E_{c.m.} = 3$ (left) and 6 MeV (right). Results obtained with NLO ${}^9\text{Be}-n$ potentials fitted to reproduce the halo ANC (green solid lines) and the non-halo one (blue dashed lines).

In addition, we have made a series of tests to study the sensitivity of the model to the choice of optical potentials between the ${}^{10}\text{Be}$ core of the projectile and the ${}^9\text{Be}$ target. The results show that, at these energies, the calculations are independent of the optical potential. This once again confirms the peripherality of the reaction and therefore the validity of the semiclassical approach, upon which the *halo-to-halo* transfer method is based. Moreover, the independence of this method to the inputs of the reaction model is a clear advantage over other techniques used so far to probe halo structures in excited nuclear states.

These tests have in particular shown no significant change when the magnitude of the imaginary part of the interaction is reduced down to 10% of its original value. This indicates that, at these sub-Coulomb beam energies, the ${}^{10}\text{Be}$ core and the ${}^9\text{Be}$ target never come close to each other. Accordingly, this excludes the possibility that, instead of the halo-neutron transfer, a deeply bound neutron is transferred from the core to the target, therefore avoiding the issue raised in Refs. [9, 4].

Experimental details

ISOLDE and MINIBALL represent the ideal combination for this ${}^9\text{Be}({}^{11}\text{Be}, {}^{10}\text{Be}){}^{10}\text{Be}^*(2^-)$ transfer reaction study. A high-intensity ${}^{11}\text{Be}$ beam is available at ISOLDE at the energies of interest for this experiment, and MINIBALL coupled with silicon detectors is the ideal detection setup for this reaction. There are a few states close to the 2^- (6.263 MeV) state: the 2_2^+ (5.958 MeV), 1_1^- (5.960 MeV) and 0_2^+ (6.179 MeV) states. Based on the previous measurement of the spectrum of ${}^{10}\text{Be}$, MINIBALL will allow for the separation of these states from the 2^- state of interest [9]. The 2^- state has a 99% branching ratio to decay via emission of a 2.895 MeV γ ray to the 2_1^+ state, which then decays to the ground state. Accordingly, we will tag on the 2.895 MeV γ rays. The efficiency of MINIBALL for the detection of the 2.895 MeV γ ray is around 3% [9]. The charged particles from this reaction will be detected by a Compact Disc (CD) double-sided silicon strip detector [17]. This detector consists of 16 annular strips of 1.9 mm while the back consists of 24 sector strips at 3.4° pitch and is subdivided into four independent quadrants. The inner and outer radii of the detectors are 9 and 41 mm respectively. A CD detector of thickness 100 μm will stop all the Be ions of interest. A Micro-Channel Plate (MCP) detector will be used to count the incoming ${}^{11}\text{Be}$ beams and will be placed 10 cm upstream of the target.

The beam intensity is expected to be 1×10^6 ion per second [18]. As stated before, two beam energies of 0.61 MeV/u and 1.22 MeV/u will be required for the measurement, corresponding to 3 MeV and 6 MeV in the c.m. frame, in order to confirm the energy dependence of this reaction. Two ${}^9\text{Be}$ targets of thickness of 0.2 and 0.6 mg/cm^2 will be used for the measurement of this reaction at 0.61 MeV/u and 1.22 MeV/u, respectively, in order to ensure the detection of the ${}^{10}\text{Be}$ particles of interest. Fig. 4 shows the kinematics of the ${}^9\text{Be}({}^{11}\text{Be}, {}^{10}\text{Be}){}^{10}\text{Be}^*(2^-)$ reaction at these two energies. Only one kinematic line is shown in Figs. 4 (a) and (b) because the two resulting ${}^{10}\text{Be}$ ions have the same kinematics. The CD detector will be positioned around 30 mm downstream of the target. It results in a laboratory angular coverage of around 16.6° to 54° , which is a tradeoff between the statistics and the twofold detection efficiency of the resulting pair of ${}^{10}\text{Be}$ ions, and is appropriate for this measurement. The coverage of the CD detector is shown as the red dashed areas in Fig. 4, which is used for estimating the statistics. Owing to the coincidence with the 2.895-MeV γ rays and the twofold coincidence of the ${}^{10}\text{Be}$, neither the particle identification nor the energy-loss/straggling of the resulting charged particles will impact the measurement. The polar angular resolution of the CD detector is around 1.6° - 3.4° in the angular range of interest, and every two strips of the CD detector will be merged into one bin for statistical estimation. Using the theoretical cross sections of the state with a halo shown in Fig. 2, the expected beam intensity, the target thickness, the coincidence efficiency of the γ -ray, and the solid angles of the CD detector, the estimated counts per hour in every two strips are plotted as a function of the laboratory angles in Fig. 5. Nine shifts will be required for each beam energy, which is determined by ensuring that every bin has at least 100 counts, which allows the statistical uncertainty within 10%. We expect to collect around 3000-5000 charged-particle+ γ coincident events for each beam energy in the proposed experiment.

The coincidence between the charged particles and the γ rays will substantially suppress the background. In addition, the angular correlation of the Be ions will be used to further isolate the transfer events from the background or other reactions. From 27° to 54° , both the resulted ${}^{10}\text{Be}$ particles from the ${}^9\text{Be}({}^{11}\text{Be}, {}^{10}\text{Be}){}^{10}\text{Be}^*(2^-)$ reaction will be detected by the CD detector, see Fig. 4 (e) and (f). The polar angular resolution of the CD detector will allow for the determination of the ${}^{10}\text{Be}$ -particle angular correlation, and therefore, the suppression of the

background from other reaction channels.

The maximum rate of the elastic-scattering events was also estimated from $\theta_{\text{lab}} = 16^\circ$ to 54° , in order to ensure that the detectors can take the expected rates. For a beam rate of around 10^6 pps, the $^{11}\text{Be}+^9\text{Be}$ elastic scattering rates in this angular range will be less than 2000 pps, which is achievable.

Summary of requested shifts:

The experimental confirmation of the presence of halos in excited nuclear state is difficult since it is not possible to apply most experimental techniques available for ground-state studies. As such, we propose a new method in which a neutron is transferred from *halo to halo*. In particular, we suggest the measurement of the $^9\text{Be}(^{11}\text{Be},^{10}\text{Be})^{10}\text{Be}^*(2^-)$ transfer reaction to investigate the possible existence of a halo in the $^{10}\text{Be}(2^-)$ excited state. Based on ADWA calculations, the presence of a halo should enhance the cross section by a factor as large as 4 compared to other excited states. At the sub-Coulomb beam energies considered here, these calculations are independent of the optical potential used, which is a clearly added value over other transfer reactions. This method will open new opportunities for future experimental studies of halos in excited states.

ISOLDE coupled to MINIBAL and a set of CD detector array seems the ideal combination to study this reaction experimentally. In total, we request **18 shifts** of beam time to measure the $^9\text{Be}(^{11}\text{Be},^{10}\text{Be})^{10}\text{Be}^*(2^-)$ reaction at 0.61 and 1.21 MeV/u, with each beam energy during 9 shifts. The ^{11}Be beam will be produced at an estimated intensity of 1×10^6 ions per second using ISOLDE. Outgoing charged particles will be detected by the CD detector array and the emitted γ rays will be detected by MINIBALL. The 2.895-MeV γ rays will be tagged for the population of the 2^- state of ^{10}Be , which allows for the isolation of other states and reaction channels. With the requested beam time, we will get at least 100 counts for each bin, which allows for a statistical uncertainty of less than 10%.

References

- [1] I. Tanihata, H. Hamagaki, O. Hashimoto, et al., Phys. Rev. Lett. 55, 2676 (1985).
- [2] P. G. Hansen and B. Jonson, Europhysics Letters 4, 409 (1987).
- [3] J. Al-Khalili and K. Arai, Phys. Rev. C 74, 034312 (2006).
- [4] K. Kuhn F. Sarazin, F. M. Nunes, et al., Phys. Rev. C 104, 044601 (2021).
- [5] J. Winfield, S. Fortier, W. Catford, et al., Nucl. Phys. A 683, 48 (2001).
- [6] S. Fortier, S. Pita, J. S. Winfield, W. N. Catford, et al., Phys. Lett. B 461, 22 (1999).
- [7] T. Aumann, A. Navin, D. P. Balamuth, et al., Phys. Rev. Lett. 84, 35 (2000)
- [8] Y. Jiang, J.-L. Lou, Y.-L. Ye, et al., Chin. Phys. Lett. 35, 082501 (2018).
- [9] J. G. Johansen, V. Bildstein, M. J. G. Borge, et al., J. Phys. G: Nucl. Part. Phys. 44, 044009 (2017).
- [10] R. C. Johnson and P. C. Tandy, Nucl. Phys. A 235, 56 (1974).
- [11] H.-W. Hammer, C. Ji, and D. R. Phillips, J. Phys. G 44, 103002 (2017).

- [12] P. Capel, D. R. Phillips, and H.-W. Hammer, *Phys. Rev. C* 98, 034610 (2018).
- [13] J. Yang and P. Capel, *Phys. Rev. C* 98, 054602 (2018).
- [14] V. Durant, P. Capel, L. Huth, A. B. Balantekin, and A. Schwenk, *Phys. Lett. B* 782, 668 (2018).
- [15] V. Durant and P. Capel, *Phys. Rev. C* 106, 044608 (2022).
- [16] M. Gennari and P. Navrátil (private communication, 2022).
- [17] A. N. Ostrowski et al., *Nucl. Instr. Meth. A* 480 (2002) 448–455.
- [18] HIE-ISODEL experiment $^{11}\text{Be}(d,p)^{12}\text{Be}$ using ISS (IS677).

Appendix

DESCRIPTION OF THE PROPOSED EXPERIMENT

The experimental setup comprises: *MINIBALL*

| Part of the | Availability | Design and manufacturing |
|-------------|--|---|
| MINIBALL | <input checked="" type="checkbox"/> Existing | <input checked="" type="checkbox"/> To be used without any modification <input type="checkbox"/> To be modified |
| | <input type="checkbox"/> New | <input type="checkbox"/> Standard equipment supplied by a manufacturer <input type="checkbox"/> CERN/collaboration responsible for the design and/or manufacturing |

HAZARDS GENERATED BY THE EXPERIMENT (if using fixed installation:) Hazards named in the document relevant for the fixed ISS installation.

Additional hazards:

| Hazards | | | |
|---------------------------------------|--|--|--|
| Thermodynamic and fluidic | | | |
| Pressure | | | |
| Vacuum | | | |
| Temperature | | | |
| Heat transfer | | | |
| Thermal properties of materials | | | |
| Cryogenic fluid | | | |
| Electrical and electromagnetic | | | |
| Electricity | | | |
| Static electricity | | | |
| Magnetic field | | | |
| Batteries | | | |
| Capacitors | | | |
| Ionizing radiation | | | |
| Target material | 9Be (0.4-1.0 mg/cm ²) | | |
| Beam particle type | ¹¹ Be | | |
| Beam intensity | 1 × 10 ⁶ | | |
| Beam energy | 0.61 and 1.22 MeV/u | | |
| Cooling liquids | | | |
| Gases | | | |
| Calibration sources: | <input checked="" type="checkbox"/> | | |
| • Open source | <input checked="" type="checkbox"/> (α calibrations source 4236RP) | | |
| • Sealed source | <input checked="" type="checkbox"/> | | |

| | | | |
|--|--|--|--|
| • Isotope | ^{148}Gd , ^{239}Pu , ^{241}Am , ^{244}Cm | | |
| • Activity | 1 kBq, 1 kBq, 1 kBq, 1 kBq = 4 kBq | | |
| Use of activated material: | | | |
| • Description | | | |
| • Dose rate on contact and in 10 cm distance | | | |
| • Isotope | | | |
| • Activity | | | |
| Non-ionizing radiation | | | |
| Laser | | | |
| UV light | | | |
| Microwaves (300MHz-30 GHz) | | | |
| Radiofrequency (1-300 MHz) | | | |
| Chemical | | | |
| Toxic | | | |
| Harmful | | | |
| CMR (carcinogens, mutagens and substances toxic to reproduction) | | | |
| Corrosive | | | |
| Irritant | | | |
| Flammable | | | |
| Oxidizing | | | |
| Explosiveness | | | |
| Asphyxiant | | | |
| Dangerous for the environment | | | |
| Mechanical | | | |
| Physical impact or mechanical energy (moving parts) | | | |
| Mechanical properties (Sharp, rough, slippery) | | | |
| Vibration | | | |
| Vehicles and Means of Transport | | | |
| Noise | | | |
| Frequency | | | |
| Intensity | | | |

| Physical | | | |
|-----------------------------|--|--|--|
| Confined spaces | | | |
| High workplaces | | | |
| Access to high workplaces | | | |
| Obstructions in passageways | | | |
| Manual handling | | | |
| Poor ergonomics | | | |

Hazard identification:

Average electrical power requirements (excluding fixed ISOLDE-installation mentioned above): N/A

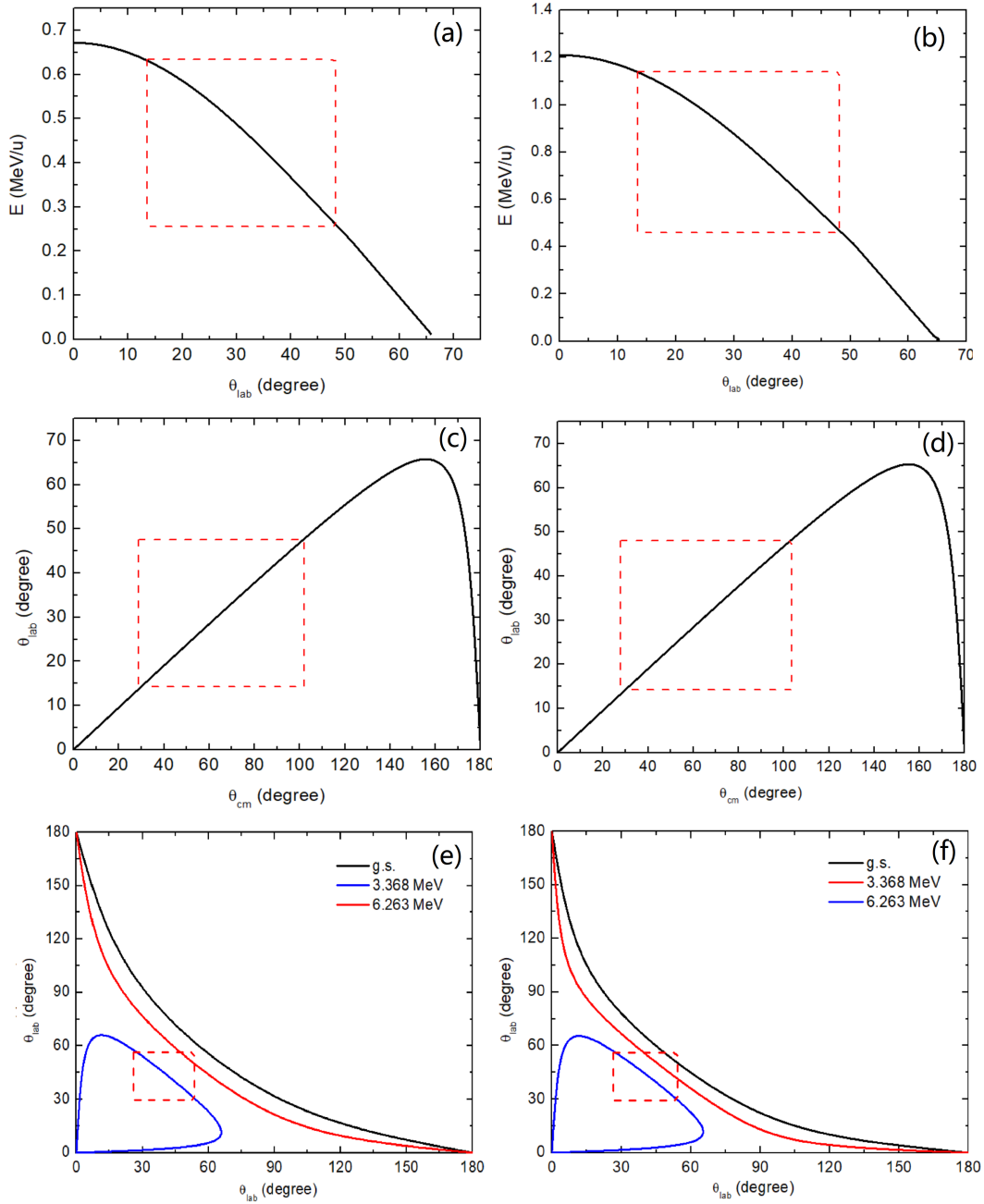


Figure 3: Kinematics of the ${}^9\text{Be}({}^{11}\text{Be}, {}^{10}\text{Be}){}^{10}\text{Be}^*(2^-)$ transfer reaction at 0.61 MeV/u (a), (c), and (e) ($E_{cm}=3$ MeV) and at 1.22 MeV/u (b), (d), and (f) ($E_{cm}=6$ MeV). The relationship of ${}^{10}\text{Be}$ energies (E) versus the laboratory angles (θ_{lab}) (a), (b) and laboratory angles (θ_{lab}) versus center of mass angles (θ_{cm}) (c), (d) are shown. The energy loss in the target has been taken into account by assuming the reaction taking place in the center of the ${}^9\text{Be}$ target. The region labeled by the red dashed lines shows the coverage the CD detector. (e) and (f) show the angular correlation of the outgoing ${}^{10}\text{Be}$ particles with population of different final states. The red dashed areas stand for the regions where both ${}^{10}\text{Be}$ particles will be detected by the CD detector.

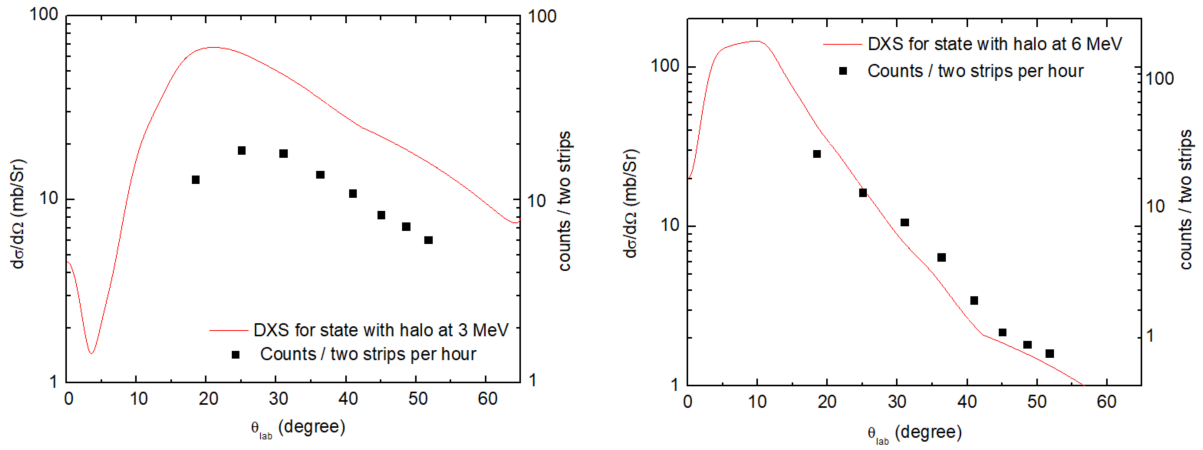


Figure 4: Red solid lines: Transfer cross sections in the laboratory frame as a function of the laboratory angles for $E_{lab} = 0.61$ (left panel) and 1.22 MeV/u (right panel). Black square dots: the estimated counts of the ${}^9\text{Be}({}^{11}\text{Be}, {}^{10}\text{Be}){}^{10}\text{Be}^*(2^-)$ transfer reaction events per hour in every two strips of the CD detector (right axis label). See text for details.